NIKHEF/97-026

ITP-SB-97-35

DESY 97-124

INLO-PUB-6/97

Comparison between the various descriptions for charm electroproduction and the HERA-data

M. Buza [1]
NIKHEF/UVA,
POB 41882, NL-1009 DB Amsterdam,
The Netherlands

Y. Matiounine
Institute for Theoretical Physics,
State University of New York at Stony Brook,
New York 11794-3840, USA

J. Smith [2]
Deutsches Electronen-Synchrotron DESY
Notkestrasse 85, D-22603, Hamburg
Germany

W.L. van Neerven
Instituut-Lorentz,
University of Leiden,
PO Box 9506, 2300 RA Leiden,
The Netherlands

July 1997

Abstract

We examine the charm component $F_{2,c}(x, Q^2, m^2)$ of the proton structure function $F_2(x, Q^2)$ in three different schemes and compare the results with the data in the x and Q^2 region explored by the HERA experiments. Studied are (1) the three flavour number scheme (TFNS) where the production mechanisms are given by the photon-gluon fusion process and the higher order reactions with three light-flavour parton densities as input (2) the four flavour number scheme (FFNS) where $F_{2,c}$ is expressed in four light flavour densities including one for the charm quark and (3) a variable-flavour number scheme (VFNS) which interpolates between the latter two. Both the VFNS and the TFNS give good descriptions of the experimental data. However one cannot use the FFNS for the description of the data at small Q^2.

[1]supported by the Foundation for Fundamental Research on Matter (FOM)

[2]on leave from ITP, SUNY at Stony Brook, New York 11794-3840, USA

The study of charm production in deep-inelastic electron-proton scattering has become an important issue in the extraction of parton densities in the proton. The reason is that the charm content $F_{2,c}(x, Q^2, m^2)$ (m is the mass of the charm quark) in the proton structure function $F_2(x, Q^2)$ has grown from around one percent in the x and Q^2 region covered by the EMC experiment [1] to around twenty-five percent in the x and Q^2 region covered by the H1 [2] and ZEUS [3] experiments at HERA. Therefore the analysis of data to yield parton densities can no longer treat charm electroproduction as a small correction.

Let us begin with a brief review of the QCD contributions to $F_{2,c}(x, Q^2, m^2)$. In lowest order (LO) the charm quark pair is produced via the photon-gluon fusion mechanism which implies that the Born contribution only contains a gluon in the initial state (extrinsic production). In next-to-leading order (NLO) we have in addition to the above reaction also Bethe-Heitler and Compton subprocesses containing the three light flavours u, d, s and their antiparticles ū, d̄, s̄ in the initial state. We will call this the three flavour number scheme (TFNS) description for charm production. The NLO calculations [4] reveal that the photon-gluon process dominates the other production mechanisms so that charm electroproduction yields a measurement of the gluon density, in particular at small x. Generalizing the TFNS to all orders in α_s we obtain the following formula for the charm content of the proton structure function

$$\begin{aligned}
F_{2,c}^{\rm EXACT}(3, x, Q^2, m^2) \;=\; & x \int_x^{z_{\rm max}} \frac{dz}{z} \Big\{ \frac{1}{3} \sum_{k=1}^{3} e_k^2 \Big[\Sigma\Big(3, \frac{x}{z}, \mu^2\Big) L_{2,q}^{\rm S}\Big(3, z, \frac{Q^2}{m^2}, \frac{m^2}{\mu^2}\Big) \\
& + G\Big(3, \frac{x}{z}, \mu^2\Big) L_{2,g}^{\rm S}\Big(3, z, \frac{Q^2}{m^2}, \frac{m^2}{\mu^2}\Big) \\
& + 3\Delta\Big(3, \frac{x}{z}, \mu^2\Big) L_{2,q}^{\rm NS}\Big(3, z, \frac{Q^2}{m^2}, \frac{m^2}{\mu^2}\Big) \Big] \Big\} \\
& + x e_c^2 \int_x^{z_{\rm max}} \frac{dz}{z} \Big[\Sigma\Big(3, \frac{x}{z}, \mu^2\Big) H_{2,q}^{\rm S}\Big(3, z, \frac{Q^2}{m^2}, \frac{m^2}{\mu^2}\Big) \\
& + G\Big(3, \frac{x}{z}, \mu^2\Big) H_{2,g}^{\rm S}\Big(3, z, \frac{Q^2}{m^2}, \frac{m^2}{\mu^2}\Big) \Big] , \qquad (1)
\end{aligned}$$

where e_c stands for the charge of the charm quark and the number of light flavours is three ($n_f = 3$). The summation variable k refers to the light quarks u,d and s. The variable z is the partonic longitudinal momentum fraction which has a maximum value $z_{\rm max} = Q^2/(Q^2 + 4m^2)$. The function Δ is the non-singlet (NS) (with respect to the flavour group) combination of light flavour densities, which are functions of the scale μ. The function Σ is the singlet (S) combination of these densities while G stands for the density of the gluon. Further $L_{2,k}$ and $H_{2,k}(k = q, g)$ represent the charm-quark coefficient functions which can also be separated into flavour singlet and flavour non-singlet parts. The functions $L_{2,k}$ describe the reactions where the virtual photon couples to the light quarks (u, d, s, ū, d̄ and s̄), whereas the $H_{2,k}$ describe the reactions where the virtual photon couples to the c (c̄) quark. Hence

$L_{2,k}$ and $H_{2,k}$ in Eq. (1) are multiplied by e_k^2 and e_c^2 respectively. Moreover, when the reaction where the photon couples to the charm quark contains a light quark in the initial state, then it can only proceed via the exchange of a gluon in the t-channel. Therefore $H_{2,q}$ is a flavour singlet. This is in contrast with $L_{2,q}$ which has both flavour singlet and non-singlet contributions. Finally we have to add to Eq. (1) that part of the proton structure function $F_2(x, Q^2)$ which contains charm quark loop contributions to the gluon self energies. The latter are only inserted in the matrix elements containing light partons (u,d,s,g). Combining this part of $F_2(x, Q^2)$ with the contributions from $L_{2,k}$ leads to the correct asymptotic behaviour of the charm quark coefficient functions at $Q^2 \gg m^2$ which allows us to perform the mass factorization discussed below. The NLO contributions to the charm quark coefficient functions were originally calculated in [4]. These functions were available analytically in the form of two-dimensional integrals which were then computed numerically. To speed up the integrations in Eq. (1) a two-dimensional grid of values for $L_{2,k}$ and $H_{2,k}$ together with an interpolation routine was provided in [5].

As a check on our exact formulae we have also calculated the asymptotic expressions for $L_{2,k}$ and $H_{2,k}$ in the limit $Q^2 \gg m^2$ [6]. These asymptotic charm quark coefficient functions contain the large logarithms of the type $\ln^i(Q^2/m^2)\ln^j(\mu^2/m^2)$ which dominate charm production far away from threshold. This has been shown in [7] by numerically comparing the asymptotic structure function defined by

$$F_{2,c}^{\mathrm{ASYMP}}(3, x, Q^2, m^2) = \lim_{Q^2 \gg m^2} \left[F_{2,c}^{\mathrm{EXACT}}(3, x, Q^2, m^2)\right], \tag{2}$$

with the exact structure function in Eq. (1). Notice that in the last equation the exact charm quark coefficient functions are replaced by their asymptotic analogues mentioned above and $z_{\max} = 1$. The NLO results [7] reveal that for $Q^2 > 20$ (GeV/c)^2 and $x < 0.01$, $F_{2,c}^{\mathrm{ASYMP}}$ coincides with $F_{2,c}^{\mathrm{EXACT}}$ which implies that the large logarithms mentioned above entirely determine deep inelastic charm production. Since these corrections vitiate the perturbation series when Q^2 gets large they should be resummed in all orders of perturbation theory. This procedure has been carried out in [7] and it consists of four steps. First we add the light parton (u,d,s,g) component of the proton structure function defined by $F_2(3, x, Q^2)$ to $F_{2,c}^{\mathrm{ASYMP}}$ in Eq. (2). Second we apply mass factorization to the asymptotic charm quark coefficient functions containing the logarithmic terms $\ln^i(Q^2/m^2)\ln^j(\mu^2/m^2)$. In this way the m^2-dependence is separated from the Q^2-dependence. The logarithms in the charm quark mass are put in the charm quark operator matrix elements whereas the logarithms in the variable Q^2 are transferred to the light parton coefficient functions denoted by $\mathcal{C}_{2,k}$ ($k = q, g$). Both quantities have been calculated up to order α_s^2 in [6], [7] and [8] respectively. In the third step we define new parton densities in a four flavour number scheme (FFNS) which can be written as convolutions of the original parton densities in the three flavour number scheme (TFNS) with the charm quark operator matrix elements mentioned above. Therefore we obtain a new parton density which represents the charm quark and is denoted by $f_{c+\bar{c}}(z, \mu^2)$. The latter has the property that it does not vanish at $\mu = m$ in the $\overline{\rm MS}$-scheme contrary to what is usually assumed in the literature. In the fourth step we rearrange terms and obtain $F_{2,c}^{\rm ASYMP}(3,x,Q^2,m^2) + F_2(3,x,Q^2) = F_2(4,x,Q^2)$ which is the FFNS result for the proton structure function. From the latter quantity one can extract the expression for the charm quark component of the proton structure function in the FFNS which will be denoted by

$$\begin{aligned} F_{2,c}^{\rm PDF}(4,x,Q^2) &= e_c^2 \int_x^1 \frac{dz}{z} \Big[f_{c+\bar c}\Big(4,\frac{x}{z},\mu^2\Big) \mathcal{C}_{2,q}^{\rm NS}\Big(4,z,\frac{Q^2}{\mu^2}\Big) \\ &\quad + \Sigma\Big(4,\frac{x}{z},\mu^2\Big) \tilde{\mathcal{C}}_{2,q}^{\rm PS}\Big(4,z,\frac{Q^2}{\mu^2}\Big) \\ &\quad + G\Big(4,\frac{x}{z},\mu^2\Big) \tilde{\mathcal{C}}_{2,g}^{\rm S}\Big(4,z,\frac{Q^2}{\mu^2}\Big) \Big] , \end{aligned} \tag{3}$$

where we have defined

$$\mathcal{C}_{2,q}^{\rm S}(n_f) = \mathcal{C}_{2,q}^{\rm NS}(n_f) + n_f \tilde{\mathcal{C}}_{2,q}^{\rm PS}(n_f) , \qquad \mathcal{C}_{2,g}^{\rm S} = n_f \tilde{\mathcal{C}}_{2,g}^{\rm S} . \tag{4}$$

The superscript PDF in Eq. (3) stands for parton density function which means that the charm component of the structure function can be completely expressed into parton densities multiplied by the light parton coefficient functions. Notice that $F_{2,c}^{\rm PDF}$ is a renormalization group invariant which implies that this structure function, like the one in Eq. (1) is explicitly independent of μ so that it becomes a physical quantity. Further it originates from the charm quark coefficient functions $H_{2,k}$ since both are proportional to e_c^2. The functions $L_{2,k}$, which are proportional to the light charge squared e_k^2, also contribute to $F_2(4,x,Q^2)$ where they increase the number of flavours by one, and provide us with order α_s^2 matching relations between the TFNS and FFNS light parton densities. The FFNS charm quark density is mainly determined by the size of the TFNS gluon density $G(3,z,\mu^2)$. Therefore the latter plays a major role in the behaviour of $F_{2,c}^{\rm EXACT}$ in Eq. (1) as well as $F_{2,c}^{\rm PDF}$ in Eq. (3). An analysis of both structure functions in [7] revealed that the former gives the best description of charm production in the threshold region where Q^2 is small and x is large. On the other hand when Q^2 is large and x is small it turns out that it is better to use $F_{2,c}^{\rm PDF}$ because it is in this region where the large logarithms $\ln^i(Q^2/m^2)\ln^j(\mu^2/m^2)$ dominate so that they have to be resummed. Therefore the TFNS is the most suitable scheme for the charm component of the structure function near threshold whereas far away from this region it turns out that the FFNS is more appropriate.

One also needs a scheme which merges the advantages of these two pictures and provides us with good description of $F_{2,c}$ in the intermediate regime in Q^2. This is given by the so called variable flavour number scheme (VFNS). In [7] we proposed the following VFNS structure function

$$\begin{aligned} F_{2,c}^{\rm VFNS}(x,Q^2,m^2) &= F_{2,c}^{\rm PDF}(4,x,Q^2) + F_{2,c}^{\rm EXACT}(3,x,Q^2,m^2) \\ &\quad - F_{2,c}^{\rm ASYMP}(3,x,Q^2,m^2) . \end{aligned} \tag{5}$$

The above expression is a generalization of Eq. (9) in [9], which was only presented in LO and has been implemented in a recent global parton density analysis [10]. (A different VFNS scheme has recently been proposed in [11].) In [9] and in [12] it was shown that $F_{2,c}^{\rm VFNS}$ in LO is less sensitive to variations in the scale μ than each term on the right-hand-side of Eq. (5) separately. Further the VFNS scheme in LO has the properties that for $Q^2 \gg m^2$, $F_{2,c}^{\rm EXACT} \to F_{2,c}^{\rm ASYMP}$ which means that $F_{2,c}^{\rm VFNS} \to F_{2,c}^{\rm PDF}$ while at low Q^2 (i.e. $Q^2 \leq m^2$) $F_{2,c}^{\rm ASYMP} \to F_{2,c}^{\rm PDF}$ so that $F_{2,c}^{\rm VFNS} \to F_{2,c}^{\rm EXACT}$. However the last relation is no longer true in higher order in α_s. The first reason is that all parton densities and the running coupling constant in $F_{2,c}^{\rm PDF}$ have four flavours whereas those appearing in $F_{2,c}^{\rm EXACT}$ and $F_{2,c}^{\rm ASYMP}$ have only three flavours. Notice that in lowest order we are allowed to put $\alpha_s(3,\mu^2) = \alpha_s(4,\mu^2)$ and $G(3,z,\mu^2) = G(4,z,\mu^2)$. Hence in LO we can use the same number of flavours in all structure functions (PDF, EXACT and ASYMP). In NLO this is no longer true, which implies that there are regions in (small) Q^2 where $F_{2,c}^{\rm ASYMP}$ cannot exactly cancel $F_{2,c}^{\rm PDF}$. The second reason is that new production mechanisms appear in NLO leading to the coefficient functions $L_{2,k}$. The latter contain the prefactor e_k^2 (e.g. the Compton process) and show up in $F_{2,c}^{\rm EXACT}$ and $F_{2,c}^{\rm ASYMP}$ but not in $F_{2,c}^{\rm PDF}$, which is proportional to e_c^2 only (see Eq. (3)). Fortunately it turns out that both these corrections are small for $Q^2 \leq m^2$ so that $F_{2,c}^{\rm VFNS,(2)} \approx F_{2,c}^{\rm EXACT,(2)}$ numerically. [3] Yet another problem arises when one chooses a parton density set in which the charm quark density vanishes at $\mu = m$. As we have found in [7] this property does not hold anymore beyond order α_s in the $\overline{\rm MS}$-scheme. This can be remedied by either making a new parton density set satisfying the conditions presented in Eqs. (2.37)-(2.41) in [7] or by choosing a different scheme. As we use charm quark densities satisfying the condition $f_{c+\bar{c}}(4,z,m^2) = 0$ then we have to make an oversubtraction, which implies that the light flavour coefficient functions $\tilde{\mathcal{C}}_{2,g}^{\rm S}$ and $\tilde{\mathcal{C}}_{2,q}^{\rm PS}$ in Eq. (3) differ from the results obtained in the $\overline{\rm MS}$-scheme.

As an application we have studied the charm component of the proton structure function in the three schemes mentioned above. The coefficient functions used for these structure functions are all computed up to order α_s^2 (see [4], [6], [8]) so that we will denote them by $F_{2,c}^{\rm EXACT,(2)}$ in Eq. (1), $F_{2,c}^{\rm PDF,(2)}$ in Eq. (3) and $F_{2,c}^{\rm VFNS,(2)}$ in Eq. (5). In Figs. 1-4 we have made plots of the x dependence of these functions for $Q^2 = 3, 12, 45$ and 170 $({\rm GeV/c})^2$ respectively and compared the results with the recent data from the H1 [2] and ZEUS [3] collaborations. We have chosen the next-to-leading log FFNS parametrization in [13] with the condition that $f_{c+\bar{c}}(z,\mu^2) = 0$ for $\mu \leq m$ for the input parton density set. Further we have taken the two-loop corrected running coupling constant with $\Lambda_4 = 200$ MeV. Notice that in principle one has to choose a TFNS parametrization for both the parton densities (see e.g [14]) and the running coupling constant for the computation of $F_{2,c}^{\rm EXACT}$ and $F_{2,c}^{\rm ASYMP}$. However we have checked that the latter are not significantly altered when we replace the parton densities in [14] by those in [13]. Finally we adopt the mass factorization scale from

[3] This is only true if we put $z_{\rm max} = 1$ for $F_{2,c}^{\rm ASYMP}$, which was not done in [7].

[9] and use

$$\mu^2 = m^2 + kQ^2(1 - m^2/Q^2)^n \quad \text{for} \quad Q^2 > m^2\,,$$
$$= m^2 \quad \text{for} \quad Q^2 \leq m^2\,, \tag{6}$$

with $k = 0.5$, $n = 2$ and $m = 1.5$ (GeV/c^2).
At $Q^2 = 3$ (GeV/c)^2 (Fig. 1) the structure function $F_{2,c}^{\rm PDF,(2)}$ is negative over the whole x-region so that we have not shown it. Nevertheless it is almost exactly equal to $F_{2,c}^{\rm ASYMP,(2)}$ so these terms cancel in Eq. (5). This means that at low Q^2 the correct description is given by $F_{2,c}^{\rm EXACT,(2)}$ (TFNS) and it is not necessary to use a VFNS. However for larger Q^2, i.e. $Q^2 \geq 12$ (GeV/c)^2, both $F_{2,c}^{\rm EXACT,(2)}$ and $F_{2,c}^{\rm PDF,(2)}$ are in agreement with most of the data. The same is true for $F_{2,c}^{\rm VFNS,(2)}$. The only exception is the value $Q^2 = 170$ (GeV/c^2) (see Fig. 4), where all descriptions are poor. The plots show the general features that $F_{2,c}^{\rm EXACT,(2)}$ (TFNS) is always below $F_{2,c}^{\rm PDF,(2)}$ (FFNS) which is due to the resummation of all the large logarithms in the latter structure function. Notice that these large terms are only included up to finite order in $F_{2,c}^{\rm EXACT,(2)}$ and $F_{2,c}^{\rm ASYMP,(2)}$. Further the results for $F_{2,c}^{\rm VFNS,(2)}$ in Eq. (5) are always between the previous curves. Finally as expected $F_{2,c}^{\rm VFNS,(2)} \approx F_{2,c}^{\rm EXACT,(2)}$ at large x (threshold region) while $F_{2,c}^{\rm VFNS,(2)} \approx F_{2,c}^{\rm PDF,(2)}$ at small x. However it is clear that one needs more precise data in finer bins of x and (large) Q^2 to discriminate between the TFNS and the FFNS in order to observe the resummation effects incorporated into $F_{2,c}^{\rm PDF,(2)}$.

Acknowledgements

The research of J. Smith and Y. Matiounine was partially supported by the contract NSF 93-09888. J. Smith would like to thank the Alexander von Humbolt Stiftung for an award to allow him to spend his Sabbatical leave in DESY.

References

[1] EMC Collaboration, J.J. Aubert et al., Nucl. Phys. B452 (1995) 109; see also B.W. Harris, J. Smith and R. Vogt, Nucl. Phys. B461 (1996) 181.

[2] H1 Collaboration, C. Adloff et al., Z. Phys. C72 (1996) 593.

[3] ZEUS Collaboration, M. Derrick et al., Phys. Lett. B349 (1995) 225; ZEUS Collaboration, M. Derrick et al., XXVII Int. Conf. on HEP '96, Warsaw (1996); ZEUS Collaboration, J. Breitweg et al., DESY-97-089.

[4] E. Laenen, S. Riemersma, J. Smith and W.L. van Neerven, Nucl. Phys. B392 (1993) 162.
B.W. Harris and J. Smith, Nucl. Phys. B452 (1995) 109.

[5] S. Riemersma, J. Smith and W.L. van Neerven, Phys. Lett. B347 (1995) 143.

[6] M. Buza, Y. Matiounine, J. Smith, R. Migneron and W.L. van Neerven, Nucl. Phys. B472 (1996) 611.

[7] M. Buza, Y. Matiounine, J. Smith, and W.L. van Neerven, hep-ph/9612398, to be published in Z. Physik C (1997).

[8] E.B. Zijlstra and W.L. van Neerven, Nucl. Phys. B383 (1992) 525.

[9] M.A.G. Aivazis, J.C. Collins, F.I. Olness and W.K. Tung, Phys. Rev. D50 (1994) 3102.

[10] H.L. Lai and W.K. Tung, Z. Phys. C74 (1997) 463.

[11] A.D. Martin, R.G. Roberts, M.G. Ryskin and W.J. Stirling, hep-ph/9612449.

[12] F.I. Olness and S. Riemersma, Phys. Rev. D51 (1995) 4746.

[13] M. Glück, E. Reya and A. Vogt, Z. Phys. C53 (1992) 127.

[14] M. Glück, E. Reya and A. Vogt, Z. Phys. C67 (1995) 433.

Figure Captions

Fig. 1. $F_{2,c}^{\rm VFNS,(2)}(x,Q^2)$ solid line and $F_{2,c}^{\rm EXACT,(2)}(x,Q^2)$ dotted line plotted as functions of x at $Q^2 = 3$ (GeV/c)^2. The experimental point is from [3].

Fig. 2. $F_{2,c}^{\rm VFNS,(2)}(x,Q^2)$ solid line, $F_{2,c}^{\rm PDF,(2)}(x,Q^2)$ dashed line and $F_{2,c}^{\rm EXACT,(2)}(x,Q^2)$ dotted line plotted as functions of x at $Q^2 = 12$ (GeV/c)^2. The experimental points are from [2] closed circles and [3] open circles.

Fig. 3. Same as Fig. 2 for $Q^2 = 45$ (GeV/c)^2.

Fig. 4. Same as Fig. 2 for $Q^2 = 170$ (GeV/c)^2.

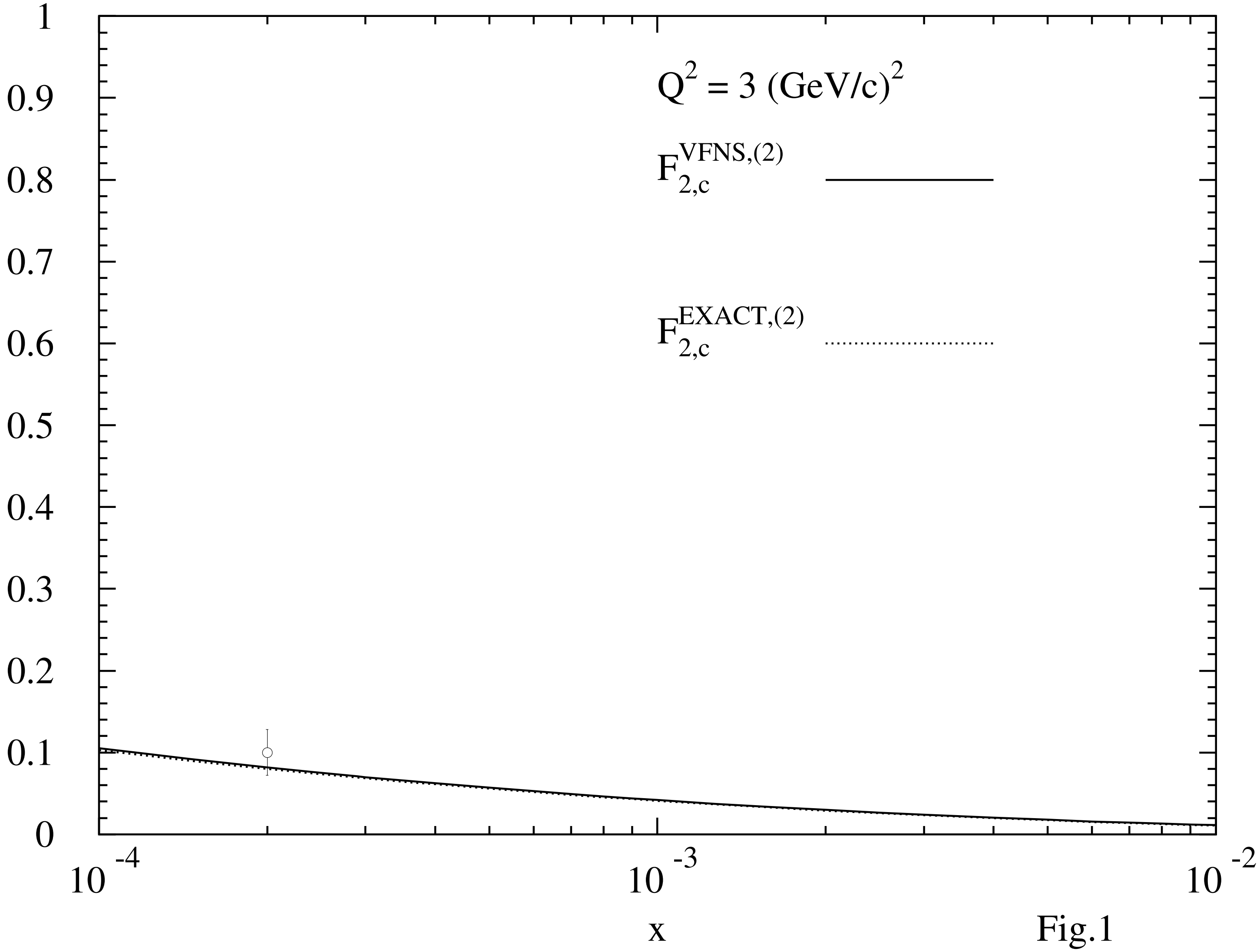

$Q^2 = 3\ (\mathrm{GeV/c})^2$
$F_{2,c}^{VFNS,(2)}$
$F_{2,c}^{EXACT,(2)}$
1
0.9
0.8
0.7
0.6
0.5
0.4
0.3
0.2
0.1
0
10^{-4}
10^{-3}
10^{-2}
x

Fig.1

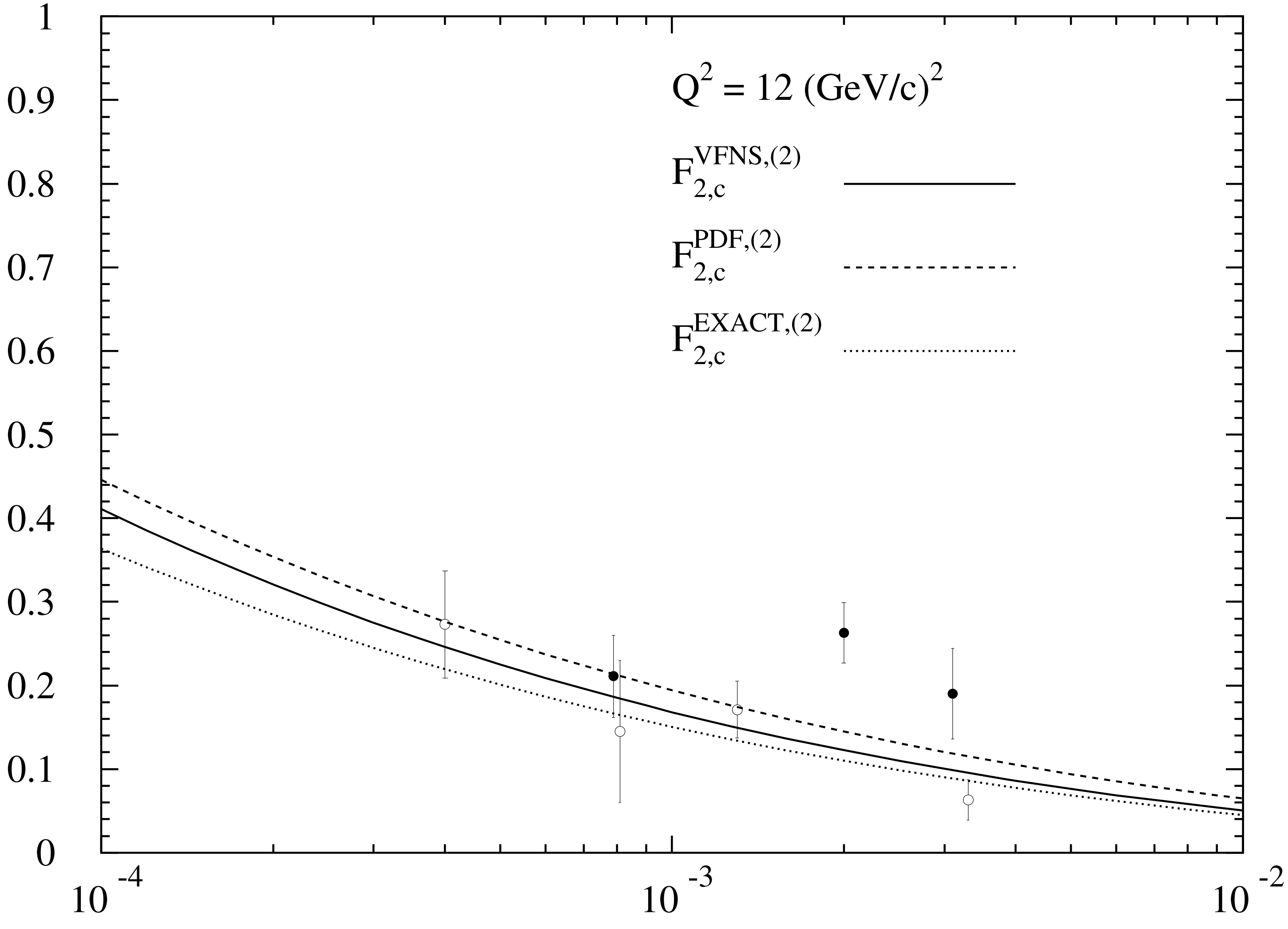

$Q^2 = 12\ (GeV/c)^2$
$F_{2,c}^{VFNS,(2)}$
$F_{2,c}^{PDF,(2)}$
$F_{2,c}^{EXACT,(2)}$
1
0.9
0.8
0.7
0.6
0.5
0.4
0.3
0.2
0.1
0
10^{-4}
10^{-3}
10^{-2}
x

Fig.2

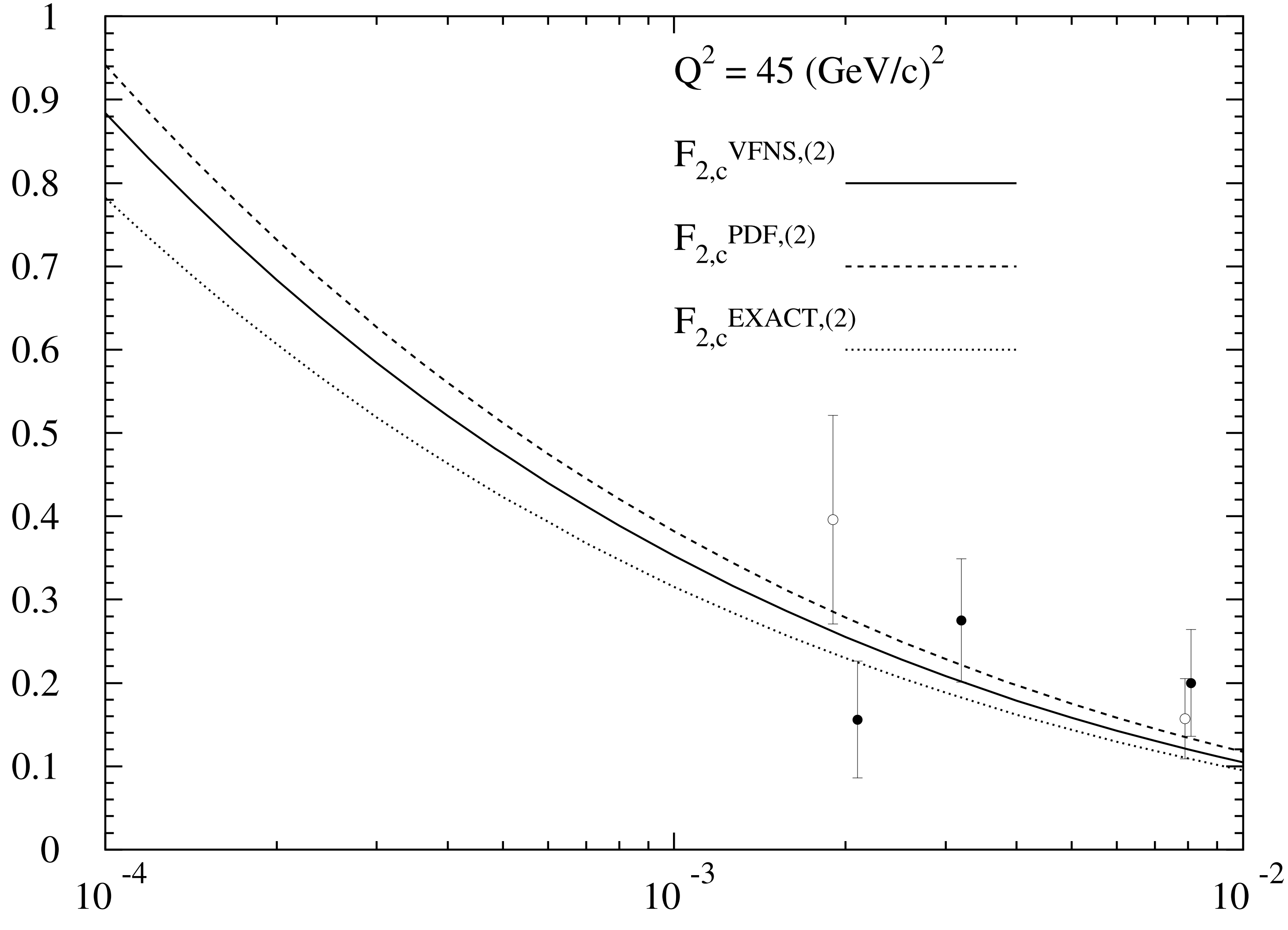

$Q^2 = 45\ (\mathrm{GeV/c})^2$
$F_{2,c}^{VFNS,(2)}$
$F_{2,c}^{PDF,(2)}$
$F_{2,c}^{EXACT,(2)}$
1
0.9
0.8
0.7
0.6
0.5
0.4
0.3
0.2
0.1
0
10^{-4}
10^{-3}
10^{-2}
x

Fig.3

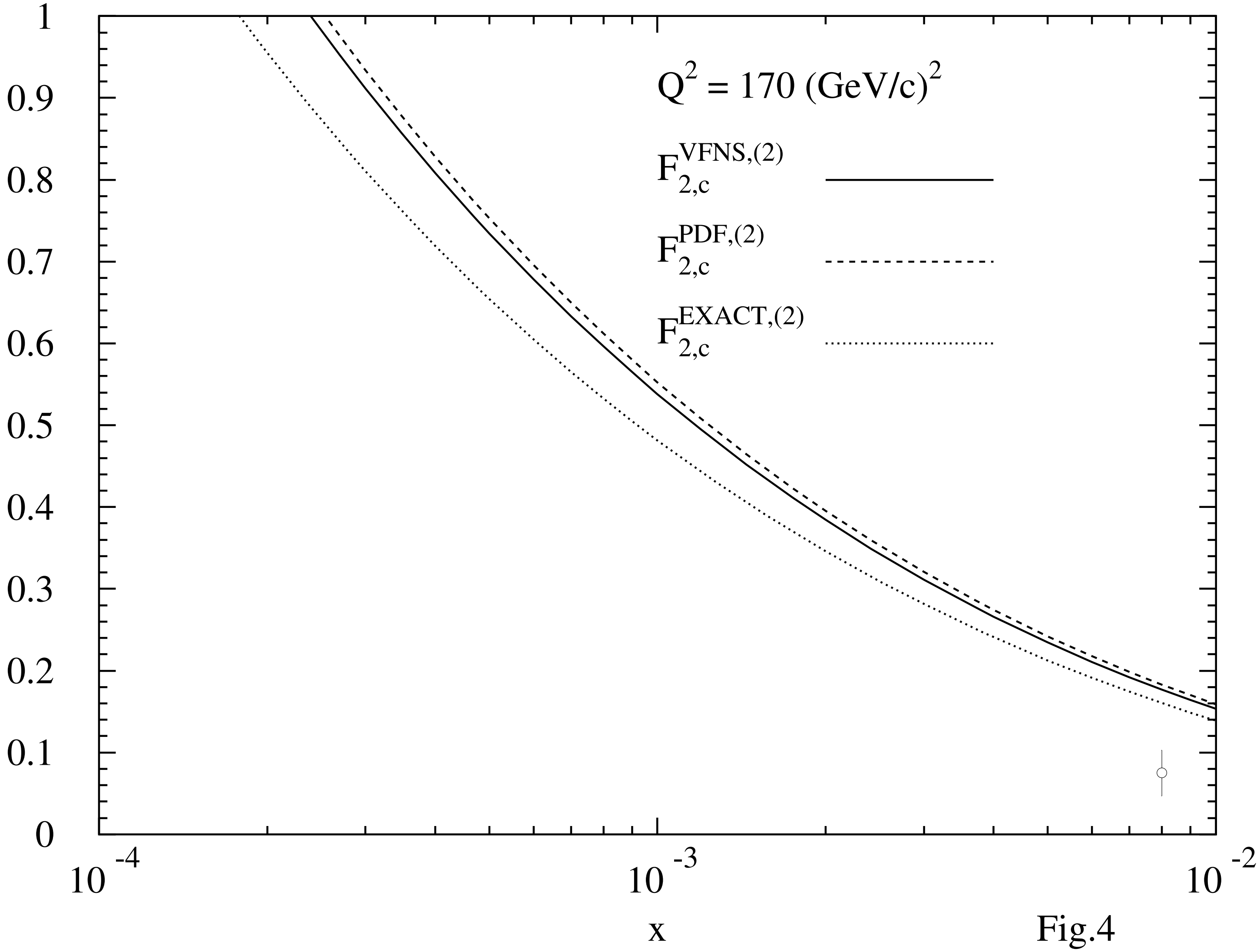

$Q^2 = 170\ (\mathrm{GeV}/c)^2$
$F_{2,c}^{VFNS,(2)}$
$F_{2,c}^{PDF,(2)}$
$F_{2,c}^{EXACT,(2)}$
1
0.9
0.8
0.7
0.6
0.5
0.4
0.3
0.2
0.1
0
10^{-4}
10^{-3}
10^{-2}
x

Fig.4